Nuclear Inst. and Methods in Physics Research, A 1031 (2022) 166595

Contents lists available at ScienceDirect

Nuclear Inst. and Methods in Physics Research, A

journal homepage: www.elsevier.com/locate/nima

A novel resistive anode using a germanium film for Micromegas detectors

Jianxin Feng, Zhiyong Zhang *, Jianbei Liu, Ming Shao, Yi Zhou

State Key Laboratory of Particle Detection and Electronics, University of Science and Technology of China, Hefei 230026, China
Department of Modern Physics, University of Science and Technology of China, Hefei 230026, China

ARTICLE INFO

Keywords:
Germanium film
Resistive anode
Micro-pattern gaseous detector
Micromegas
Discharge suppression

ABSTRACT

A germanium film manufactured by vacuum evaporation was studied and used as a novel resistive anode in Micromegas detectors. Its sheet resistivity characteristics, particularly the thickness dependence and long-term evolution of the film, were demonstrated. Resistive anodes help to suppress the discharge of the detector, but also degrade its counting rate capability. For this reason, a fast grounding method to maintain the rate capability was developed and tested. Micromegas prototypes using the germanium anode were tested and verified. The results indicate that the germanium anode can be a good option not only for Micromegas but also for other micro-pattern gaseous detectors.

1. Introduction

The micro-mesh gaseous structure (Micromegas) has been significantly developed in the past few decades since it was invented in 1996 [1]. As a typical micro-pattern gaseous detector (MPGD), Micromegas also suffers from issues with discharges. The resistive anode has been verified to be a good solution and has been widely studied to deal with discharges. Innovative methods to fabricate resistive anodes using various materials have been investigated, such as, screen printing for a resistive paste ([1]RP), which is usually a mixture of epoxy glue and carbon powder; magnetron sputtering for graphite targets to construct diamond-like carbon (DLC) [2], and so on. Inspiring results have been reported on RP [3,4] and DLC [5,6]. However, there are still some problems to overcome in order to apply these resistive approaches. For instance, an RP anode is not sufficiently robust enough so that its surface material may be sputtered when a sparking event occurs in a detector. It is also difficult to achieve high resistivity and large area uniformity up to tens of megohms per square. On the other hand, it is not easy to manufacture DLC over a large-area, rigid plane such as an FR-4 board, which is most commonly used as the readout printed circuit board (PCB) in MPGDs.

Therefore, to address these gaps, this study investigates a germanium (Ge) film-based resistive anode, which can be easily manufactured using vacuum evaporation [7,8] and extended to cover a large area on a PCB substrate. Additionally, owing to the good correlation between sheet resistivity and the thickness of the Ge film, an appropriate resistivity value can be obtained for practical applications.

2. Ge film for resistive anode

2.1. Manufacturing method

The resistive anode was coated with a Ge film in a conventional stainless steel chamber at a pressure of $\sim 1 \times 10^{-4}$ Pa using thermal evaporation via an electromagnetic heater or an electron beam. The Ge source was a ~50 Ω cm single crystal of 99.9999% purity. The evaporator was a tungsten boat. Even though the volume resistivity of Ge is low, a sheet resistivity varying from MΩ/□ to GΩ/□ can be obtained by tuning the thickness of the Ge film. When using a sheet-type resistive anode, an insulating layer is necessary to separate the resistive layer and the readout copper strips as shown in Fig. 1. The signals are read out from the strips by capacitive coupling. The strips were fabricated in the middle layer by a standard PCB process, where an FR-4 layer with a maximum thickness of ~80 μm covering the strips was used as the insulating layer. Then, the Ge films were coated on the FR-4 substrate and grounded through some grounding nets, which will be discussed further in Section 4.1.

Abbreviations: DLC, diamond-like carbon; MPGD, micro-pattern gaseous detector; PCB, printed circuit board; RMS, root mean square; RP, resistive paste; TBM, thermal bonding method

* Corresponding author at: State Key Laboratory of Particle Detection and Electronics, University of Science and Technology of China, Hefei 230026, China.
E-mail address: zhzhy@ustc.edu.cn (Z. Zhang).

[1] Polymer resistors, product-category. https://www.ferro.com. <https://www.ferro.com/-/media/files/resources/electronic-materials/ferro-electronic-materials-rs121xx-series-polymer-resistors.pdf>.

[2] Hioki-SM7120. https://www.techedu.com, <https://res.cloudinary.com/iwh/image/upload/q_auto,g_center/assets/1/26/Hioki_SM71xx_Series_User_Manual.pdf>.

https://doi.org/10.1016/j.nima.2022.166595
Received 6 December 2021; Received in revised form 12 February 2022; Accepted 7 March 2022
Available online 18 March 2022

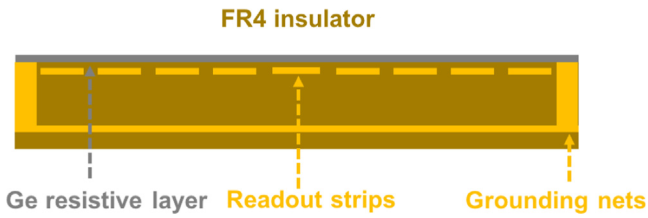

Fig. 1. Schematic of Ge films manufactured on the readout PCB.

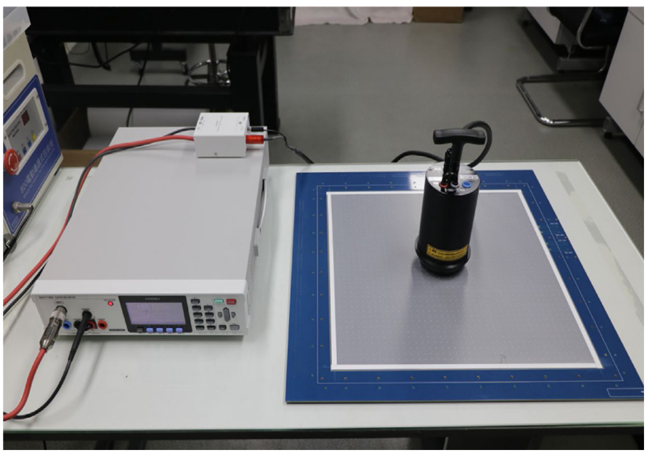

Fig. 2. Resistivity test of the Ge samples.

2.2. Performance of the Ge films

In order to study the performance of the resistive Ge anode, six Ge film samples with an effective area of 40 × 40 cm^2 were coated on the FR-4 substrate. The film thicknesses were 100 nm, 200 nm, 300 nm, 400 nm, 600 nm, and 1000 nm. A [2]HIOKI SM7120 high resistance meter (Fig. 2) was used to monitor the resistivity over a long period of approximately 12 months. Ge anode samples were observed to have deteriorated severely in humid conditions: the surface blackened and the sheet resistivity rose sharply in an uncontrollable way. Therefore, the samples were stored in a dry air cabinet with humidity control. Both temperature and humidity were monitored during the test, and the relative humidity, ratio between the absolute and saturation humidity given the same temperature was tuned to ∼20%.

First, the non-uniformities of sheet resistivity, all of the six samples were measured at a distance of every 4 cm and for a total of 81 test points. Non-uniformity is the ratio of the root mean square (RMS) of the test points to their average. Fig. 3 illustrates the 2D sheet resistivity distribution of 6.7% non-uniformity for the best sample, the average value of which is 35.2 MΩ/□ and the corresponding RMS is 2.31 MΩ/□. Other samples with different sheet resistivity have similar non-uniformities, ranging from 11.3% to 13.6%. A non-uniformity below 15% is reproducible with current evaporation technology.

The sheet resistivity of the samples was tested in the middle position every 3 or 4 days. Changes in resistivity with time are shown in Fig. 4. During the first 60 days, the Ge surface was gradually oxidised, and the sheet resistivity slowly increased to be 2–3 times higher than the initial values. Then, an oxide passivation layer was formed, and the resistivity became stable. The residual variations in sheet resistivity were likely due to fluctuations in the temperature.

Fig. 5 shows the average sheet resistivity after 60 days for Ge films with different thicknesses, error bars represent the root mean square of the resistivity. An anti-correlation between the sheet resistivity and the thickness could clearly be seen. It was concluded that the sheet

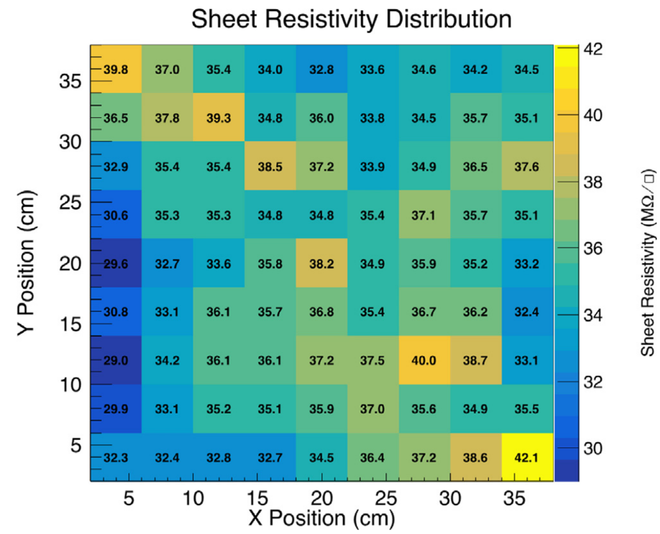

Fig. 3. 2D sheet resistivity distribution of the 40 cm × 40 cm Ge film sample with the best uniformity.

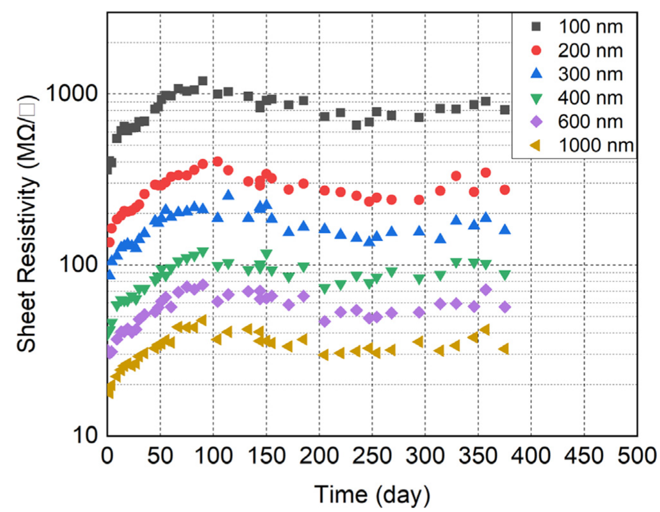

Fig. 4. Sheet resistivity changes as a function of time for different thicknesses of Ge films.

resistivity can be adjusted in a range of tens of MΩ/□ to ∼GΩ/□ by tuning the thickness of the Ge film from 1000 nm to 100 nm, which satisfies the requirements of most MPGDs. A relatively low resistivity is helpful when a good spatial resolution with a wide strip pitch is required [4,9], while a high one is useful for improving the spark-resistant capability, thus making the detector more stable.

3. Performance of Ge anode-based detector

Many Micromegas prototypes with the Ge film anode were fabricated using the thermal bonding method (TBM), which has been developed for fabricating Micromegas detectors [10]. Fig. 6 shows a photo of a readout PCB coated with a ∼400-nm-thick Ge film. The Ge film was coated by thermal evaporation and grounded using the border grounding method (Section 4.1). These prototypes have been studied with 5.9 X-rays in an argon (7% CO_2)-based environment, and a good energy resolution (∼16%) and a high gas gain (up to 1 × 10^5) were obtained [10].

The discharge rate was tested with 8.0 keV X-rays at a detector gain of approximately 8000 for a duration of 26.3 h. A Keithley (6482)

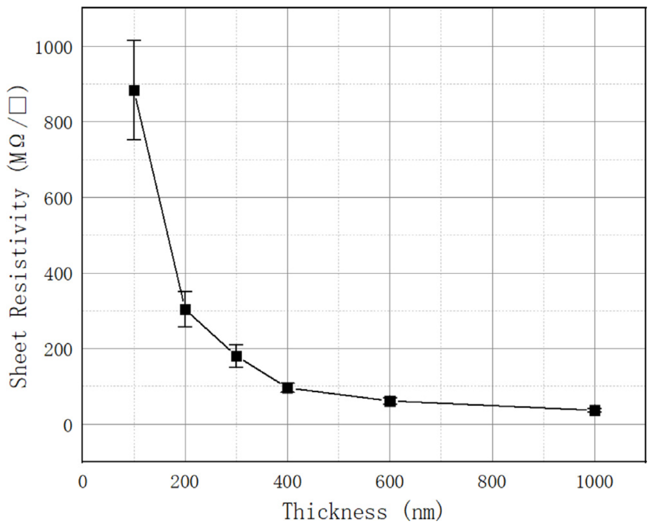

Fig. 5. Average sheet resistivity with varying thicknesses of Ge films.

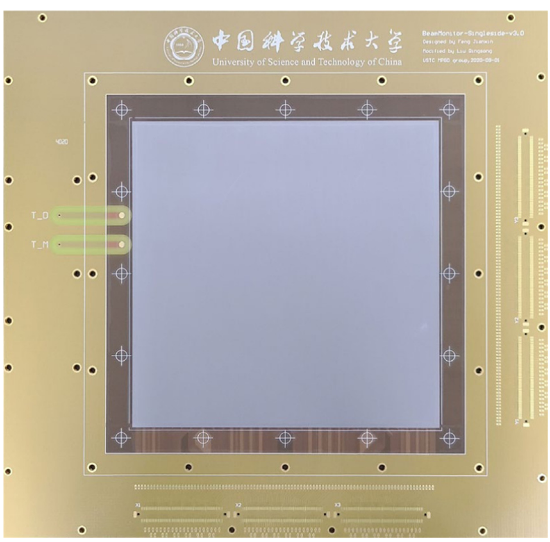

Fig. 6. Photograph of Ge-coated PCB, where the 15×15 cm^2 grey area is the Ge anode grounded at the edges, and the readout strips are manufactured in the middle layer covered by an insulated FR-4 layer.

picoammeter was used to measure the mesh currents with a resolution of 10 fA at ±20 nA dynamic range. Current divergences larger than 10σ from the average were considered as a spark event. The current (baseline) profile was a Gaussian distribution whose mean value was −0.73 nA with $\sigma = 0.089$ nA. The discharge rate was finally calculated as 5.1×10^{-8}, after dividing the discharge events by the X-ray counts in the test period. The detector current distribution over time is shown in Fig. 7. There are two large sparks whose currents exceed the lower limit of the Y-axis, corresponding to current fluctuations of about 400 nA and 40 nA respectively. The lower Y-axis limit is selected to present the current more clearly. The high gain and low sparking rate indicate the excellent performance of this Ge film anode.

Furthermore, the rate capability at the centre of the 15×15 cm^2 active region was also studied with an 8.0 keV Cu-target X-ray gun. The results and a comparison with the grid-dot grounding method are presented in Section 4.3.

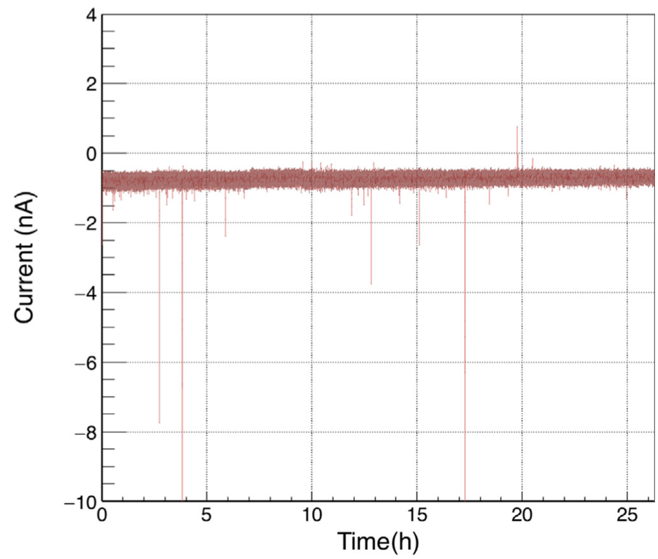

Fig. 7. Detector current variations in a test duration of 26.3 h.

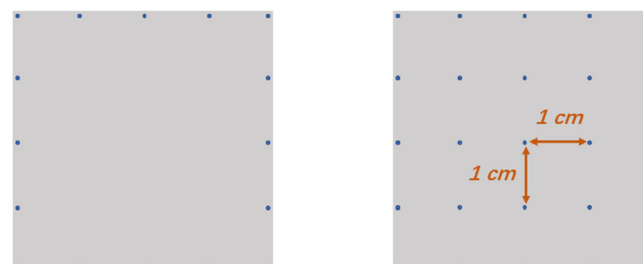

Fig. 8. Schematic of grounding methods. Left: border grounding; right: grid-dot grounding.

4. Grounding methods towards high counting rate application

4.1. Grounding methods for the Ge anode

When using this sheet-type resistive anode in MPGDs, a decrease in the counting rate is inevitable when reducing the sparking rate. In this regard, a good grounding method for the Ge film will help maximise its counting rate capability. In this work, two grounding methods, called border grounding and grid-dot grounding, were used and tested with Micromegas detectors.

As shown in Fig. 8, in the case of the border grounding method (left), the Ge film is connected to the anode potential (usually grounded) at its border through an array of copper dots that are fabricated in the PCB. In the case of the grid-dot grounding method (right), the Ge film is connected to the anode potential (a grounding net) through grid-distributed copper dots, which are arranged in a sensitive area at an appropriate pitch of ~10 mm. The border grounding method is relatively simple, suitable for some applications where the counting rate is not too high, such as cosmic ray tests, rare event searching, etc. In comparison, the grid-dot grounding method can be used to realise an extremely high counting rate.

4.2. Micromegas detector with grid-dot grounding Ge anode

As mentioned above, metal dots distributed in a grid are used to connect the Ge film at a pitch of approximately 10 mm. The metal dots are usually less than 0.5 mm in diameter and appropriately covered by 1 mm diameter spacers used in Micromegas detectors manufactured by the TBM to avoid sparks around them. Fig. 9 shows a schematic

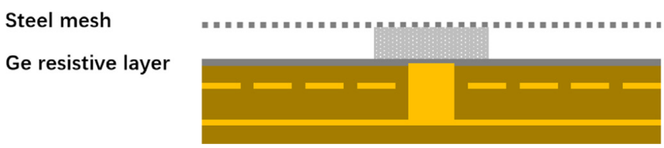

Fig. 9. Schematic diagram of the method used to cover the grid-distributed grounding dots.

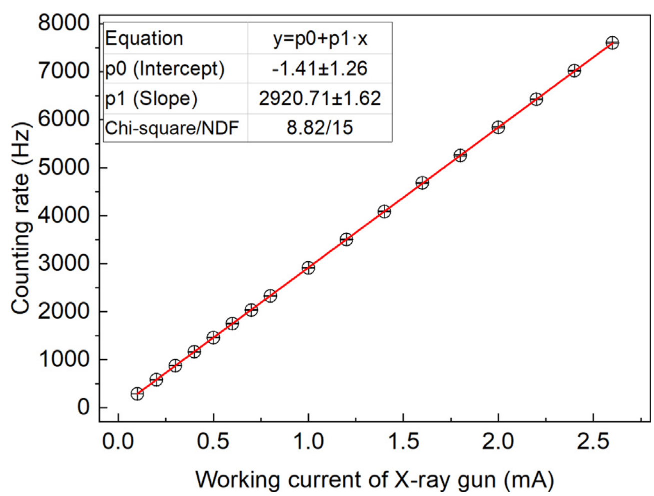

Fig. 10. Linear correlation between the working current of the X-ray gun and the counting rate of the detector.

diagram of the method using the TBM to cover the grid-distributed grounding dots without increasing additional dead area. This method was also used to fabricate a Micromegas prototype with an active area of 15 × 15 cm^2 to study its counting rate.

4.3. Counting rate test

A test system was set up to evaluate the counting rate of the Micromegas detectors using different grounding methods. The detectors were irradiated with X-rays, which were collimated by a 10-cm-long copper tube with a diameter of 8 mm. The collimator is set very close to the detector window, so the beam spot diameter is considered to be 8 mm.

Before the counting rate test, the linear correlation between the recorded counting rate (R_x) of the detector and the working current (I_x) of the X-ray gun was calibrated at relative low X-ray flux, as shown in Fig. 10, therefore the R_x when exceeding the capability of the counting readout electronics could be calculated by the formula of $R_x = p1 \cdot I_x + p0$, where the p0, p1 are the intercept and slope parameters of the linear fit. In this calibration, the counting rate of the detector was measured from its mesh signal. The mesh signals were first amplified by a fast timing preamplifier with a rise time of <12 ns at 100 pF (the timing output of the ORTEC 142AH module). They were then further amplified by a spectroscopy amplifier with a shaping time of 0.5 μs (CAEN N968 module) and discriminated by a leading-edge discriminator (CAEN N840 module) with a maximum input frequency of 80 MHz. They were finally counted by a counter (CAEN N1145 module), which also had a maximum frequency of 80 MHz.

In the counting rate test, the relative gas gain was monitored by measuring the mesh current and normalising it by the value at a low irradiation condition (∼10 kHz, corresponding gain of ≈6000). Fig. 11 shows the normalised gain changing as a function of the counting rate for different grounding cases.

The gas gain drops 10% and reaches 0.44 MHz/cm^2 for the grid-dot grounding case (black symbols) and > 0.13 MHz/cm^2 for the border grounding case (blue symbols). The grid-dot grounding method is excellent at charge evacuation spreading on the resistive layers and is suitable for large detectors.

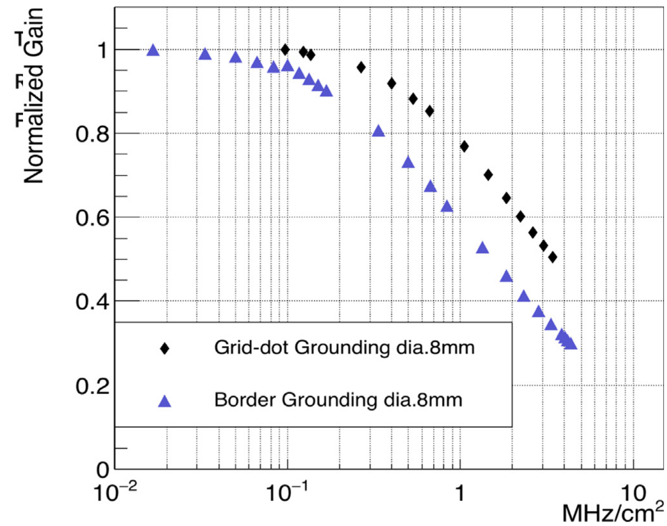

Fig. 11. Comparison of counting rates for different grounding techniques.

5. Conclusion

A new method to manufacture resistive anodes using Ge films for MPGDs was described in detail, and its features of thickness dependence and stability of the resistivity were studied. The newly explored resistive anode material combined a practical production technique make it adoptable for diverse gaseous detectors. Micromegas detectors fabricated with this Ge film-based anode were also tested, and a high gain above 10^5 and a low sparking rate were obtained, indicating the excellent performance of this type of resistive anode. Two different grounding methods, border grounding and grid-dot grounding, were proposed and tested with Micromegas prototypes. A high counting rate capability (> 100 kHz/cm^2) was verified using an 8.0 KeV X-ray source. In summary, Ge films are easy to manufacture in the laboratory and have good performance characteristics for use in resistive anodes of MPGDs, making them an attractive choice for future research.

Furthermore, many Micromegas detectors using this Ge films have been fabricated and applied to different experimental applications, for instance, used for investigation of the thermal-bonding method [10], for neutron detector [11], tracker detector [12] and TPC readout [13] etc. Thus its performance was verified in practical applications.

In addition, it should be noted that the Ge films must be stored well in dry, low-temperature (short-term heating within a few minutes is acceptable in the TBM) environments to prevent oxidation.

CRediT authorship contribution statement

Jianxin Feng: Validation, Methodology, Investigation, Formal analysis, Data curation, Writing – original draft, Writing – review & editing. **Zhiyong Zhang:** Conceptualization, Methodology, Investigation, Writing – review & editing, Supervision, Project administration, Resources, Funding acquisition. **Jianbei Liu:** Writing – review & editing, Supervision, Project administration, Resources, Funding acquisition. **Ming Shao:** Writing – review & editing. **Yi Zhou:** Writing – review & editing.

Declaration of competing interest

The authors declare that they have no known competing financial interests or personal relationships that could have appeared to influence the work reported in this paper.

Acknowledgements

The authors wish to thank the Hefei Comprehensive National Science Center for their support. This work was partially performed at the University of Science and Technology of China (USTC) Center for Micro and Nanoscale Research and Fabrication, and we thank Yu Wei for his help in the nanofabrication steps of the Ge coating and Dianfa Zhou for his help in the laser cutting of the thermal spacers.

Funding

This work was supported by the Program of National Natural Science Foundation of China [grant numbers 11935014, 12075238, and 11605197], National Key Programme for S&T Research and Development, China [grant number 2016YFA0400400], USTC Research Funds of the Double First-Class Initiative, China [grant number YD2360002002], Fundamental Research Funds for the Central Universities, China [grant number WK2360000011 and WK2360000010], and the State Key Laboratory of Particle Detection and Electronics, China, [grant number SKLPDE-ZZ-202109].

References

[1] Y. Giomataris, et al., MICROMEGAS: a high-granularity position-sensitive gaseous detector for high particle-flux environments, Nucl. Instrum. Methods Phys. Res. A 376 (1996) 29–35, http://dx.doi.org/10.1016/0168-9002(96)00175-1.

[2] J. Robertson, Diamond-like amorphous Carbon, Mater. Sci. Eng. R 37 (2002) 129–281, http://dx.doi.org/10.1016/S0927-796X(02)00005-0.

[3] T. Alexopoulos, et al., A spark-resistant bulk-micromegas chamber for high-rate applications, Nucl. Instrum. Methods Phys. Res. A 640 (2011) 110–118, http://dx.doi.org/10.1016/j.nima.2011.03.025.

[4] T. Alexopoulos, et al., Construction techniques and performances of a full-size prototype micromegas chamber for the ATLAS muon spectrometer upgrade, Nucl. Instrum. Methods Phys. Res. A 955 (2020) 162086, http://dx.doi.org/10.1016/j.nima.2019.04.040.

[5] G. Bencivenni, et al., Performance of μ-RWELL detector vs resistivity of the resistive stage, Nucl. Instrum. Methods Phys. Res. A 886 (2018) 36–39, http://dx.doi.org/10.1016/j.nima.2017.12.037.

[6] Y. Zhou, et al., Fabrication and performance of a μ RWELL detector with diamond-like carbon resistive electrode and two-dimensional readout, Nucl. Instrum. Methods Phys. Res. A 927 (2019) 31–36, http://dx.doi.org/10.1016/j.nima.2019.01.036.

[7] Y. Sakai, K. Takahashi, Preparation and properties of vacuum-deposited germanium thin films, Japan. J. Appl. Phys. 2 (1963) 629–636, http://dx.doi.org/10.1143/JJAP.2.629.

[8] R. Bellazzini, et al., A two-step parallel plate chamber with a resistive germanium anode and a two dimensional readout for the detection of minimum ionizing particles, Nucl. Instrum. Methods Phys. Res. A 252 (1986) 453–457, http://dx.doi.org/10.1016/0168-9002(86)91222-2.

[9] J. Manjarrés, et al., Performances of anode-resistive Micromegas for HL-LHC, J. Instrum. 7 (2012) C03040, http://dx.doi.org/10.1088/1748-0221/7/03/C03040.

[10] J. Feng, et al., A thermal bonding method for manufacturing micromegas detectors, Nucl. Instrum. Methods Phys. Res. A 989 (2021) 164958, http://dx.doi.org/10.1016/j.nima.2020.164958.

[11] B. Qi, et al., Measurement of the neutron beam profile of the Back-n white neutron facility at CSNS with a Micromegas detector, Nucl. Instrum. Methods Phys. Res. A 957 (2020) 163407, http://dx.doi.org/10.1016/j.nima.2020.163407.

[12] Y. Wang, et al., A high spatial resolution muon tomography prototype system based on micromegas detector, IEEE Trans. Nucl. Sci. 69 (1) (2022) 78–85, http://dx.doi.org/10.1109/TNS.2021.3137415.

[13] J. Pan, et al., An ultra-low background alpha detection system with micromegas-based time projection chamber, Rev. Sci. Instrum. 93 (2022) 013303, http://dx.doi.org/10.1063/5.0070612.